

HETEROCYCLES, Vol. 102, No. 9, 2021, pp. 1767 - 1778. © 2021 The Japan Institute of Heterocyclic Chemistry
Received, 12th March, 2021, Accepted, 21st June, 2021, Published online, 7th July, 2021
DOI: 10.3987/COM-21-14454

APPLICATION OF A NEW 4'-FUNCTIONALIZED 2,2':6',2''-TERPYRIDINE RUTHENIUM(II) COMPLEX AS A SENSITIZER IN DYE SENSITIZED SOLAR CELLS

Azam Nasirian,^{1*} Valiollah Mirkhani,^{1*} Majid Moghadam,^{1*} Shahram Tangestaninejad,¹ and Iraj Mohammadpoor-Baltork¹

¹Department of Chemistry, Catalysis Division, University of Isfahan, 81746-73441, Isfahan, Iran

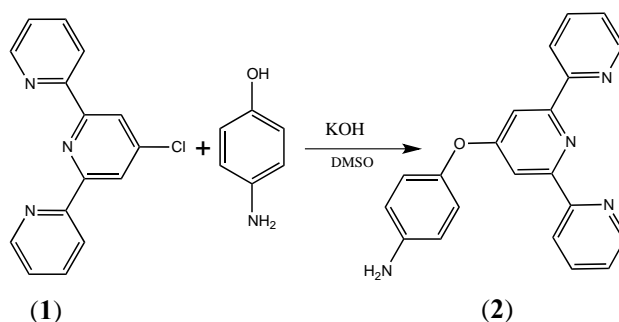
*Corresponding author: E-mail: aazamnasirian@gmail.com, mirkhani@sci.ui.ac.ir; moghadamm@sci.ui.ac.ir

Abstract – In this work, the synthesis of a Ru(II) complex derived from 4'-functionalized 2,2':6',2''-terpyridine ligand was described and the its spectral property of this complex was investigated. We synthesized this ligand and used that for the synthesis of Ru(II) complex. Ligand and complex were characterized by UV-vis, FT-IR, ESI-MS, CHN analysis and NMR methods. After synthesis and characterization of this complex, we investigated the application of this complex as a photosensitizer in manufacturing of dye-sensitized solar cells. A sandwich cell was prepared using the dye anchored TiO₂ film as a working electrode and a second conducting glass coated with chemically deposited platinum as a counter electrode. The application of this complex in a dye-sensitized nanocrystalline TiO₂ solar cell has demonstrated a short-circuit current density of 12.84 mA, with an open circuit potential of 0.69 V. The total efficiency of this dye-sensitized solar cell with this complex was 4.97%.

Metal oxides have a wide-bandgap called semiconductor. In solar cells, the surface of these semiconductors is functionalized by attaching transition-metal complexes. These semiconductors are very important in solar energy conversion in dye-sensitized solar cells and molecular electronics.^{1,2} Dye-sensitized solar cells (DSSCs) have lately received great consideration because of their easy manner of fabrication and productiveness in relation to the cost compared with silicon (Si) based photovoltaic cells.^{3,4} Terpyridine ligands that used for the synthesis of metal complexes with different transition metal

ions have a lot of applications in different fields such as nanoscience and photochemistry.⁵ The 2,2':6',2''-terpyridine and its derivatives are very important and they have been used as building blocks for supramolecular structures such as polymers, micelles and dendrimers.⁵⁻¹³ Functionalized terpyridine ligands have been anchored to TiO₂, gold or silica-titania surfaces to build monolayer or semiconductors, and their energy transfer has been investigated.¹⁴⁻²³ Ruthenium(II) complexes have received particular consideration in dye-sensitized solar cells.¹⁴ Metal-complexes bearing terpyridine ligands with spacers at 4'-position, provide a means of directionality, and so a means of linear communication, it means that the electronic communication can occur along the coordination axis and insertion of a single substituent in the 4'-position of the terpyridine ligand causes no enantiomeric derivatives compared to bipyridine derivatives, and therefore, the functionalization of terpyridine ligand is very important. Several attempts have been done to the structural variation of the Ru complexes in order to obtain sensitizers showing increased absorption coefficients for enhanced light conversion.²⁴⁻²⁶ In general, Ru polypyridyl sensitizers show appropriate absorption coefficients in the wavelength domain between 400–600 nm. In this work, we focused our attention on these wavelengths or longer wavelengths, where insufficient light absorption of Ru sensitizers limits its performance in dye-sensitized solar cells. So, we attempted to prepare a Ru complex for increasing the performance of DSSCs. We synthesized a 4'-functionalized 2,2':6',2''-terpyridine ligand and its Ru complex, used it as a dye in manufacturing of dye-sensitized solar cell, and finally its efficiency was measured.

The synthesis of 4'-(4-aminophenyl)-2,2':6',2''-terpyridine (**2**) from 4'-chloro-2,2':6',2''-terpyridine (**1**) and 4-aminophenol is summarized in Scheme 1. So, in the presence of KOH, 4-aminophenol was treated with **1** in DMSO to produce **2**.



Scheme 1. Synthetic route of compound (**2**)

The compound **3** was produced when 2,4-pentanedione was added to a flask containing 4-iodobenzoic acid, CuI, K₂CO₃ and *L*-proline in DMSO solvent under N₂ gas and the mixture was heated at 90 °C (Scheme 2).

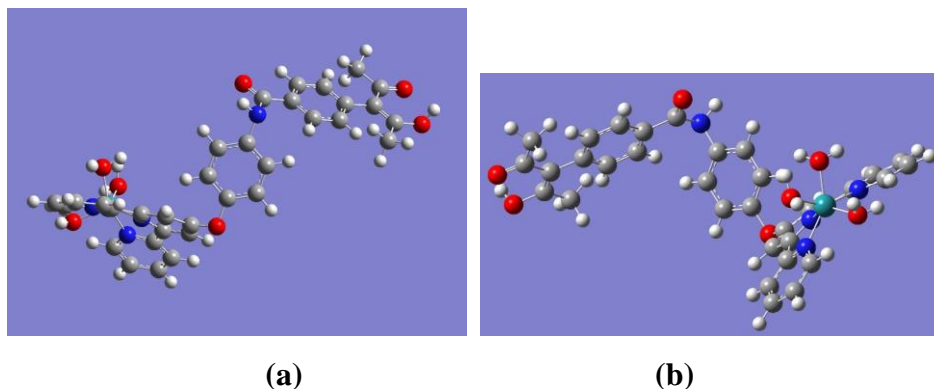


Figure 1. (a) Synthetic route of compound (5); (b) Structures of complex 5

The TiO₂ thin film was prepared using the doctor blade process and immersed in the synthesized Ru complex solution, dye sensitization was performed, and the TiO₂ film was washed with ethanol multiple times before being measured (Figure 2).

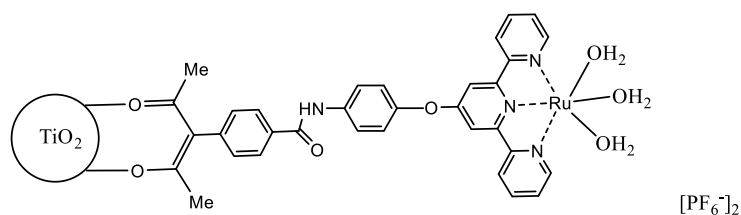


Figure 2. TiO₂ thin film preparation

The UV–vis spectrum of complex **5** in acetonitrile exhibits clearly the typical metal to ligand charge transfer (MLCT) transition of the Ru(II)–terpyridine complex at $\lambda_{\text{max}} = 325$ nm and 540 nm (Figure 3).

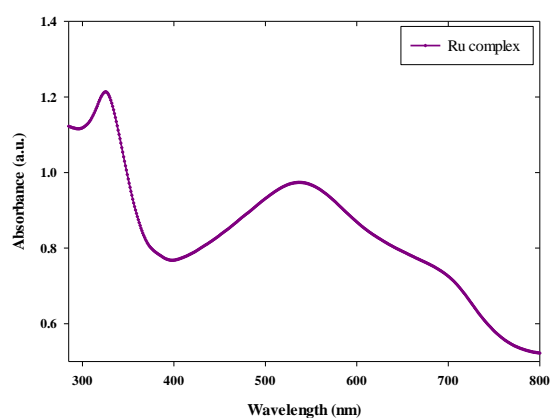


Figure 3. UV–Vis spectrum of Ru complex in MeCN solution (0.4 M)

The B3LYP functional with the def2svp basis set was used to optimize the geometry and The HOMO and LUMO molecular orbitals of complex at the DFT level calculation. Figure 4 shows the optimal geometry of complex. The molecular orbitals of this compound are developed in order to understand more about the nature of this complex with def2tzvpp basis set. Electrical and optical characteristics are influenced by the HOMO and LUMO orbitals. Only the molecular orbital of these two states was determined to be more relevant (see Figure 5). The computed energies of the frontier molecular orbitals HOMO and LUMO are 5.19888 eV and 3.17840 eV, respectively, as shown in Figure 5. The gap energy is 2.02 eV, which is correct. This number permits this hybrid compound to be classified as a semiconductor with a strong potential for application in photovoltaics.

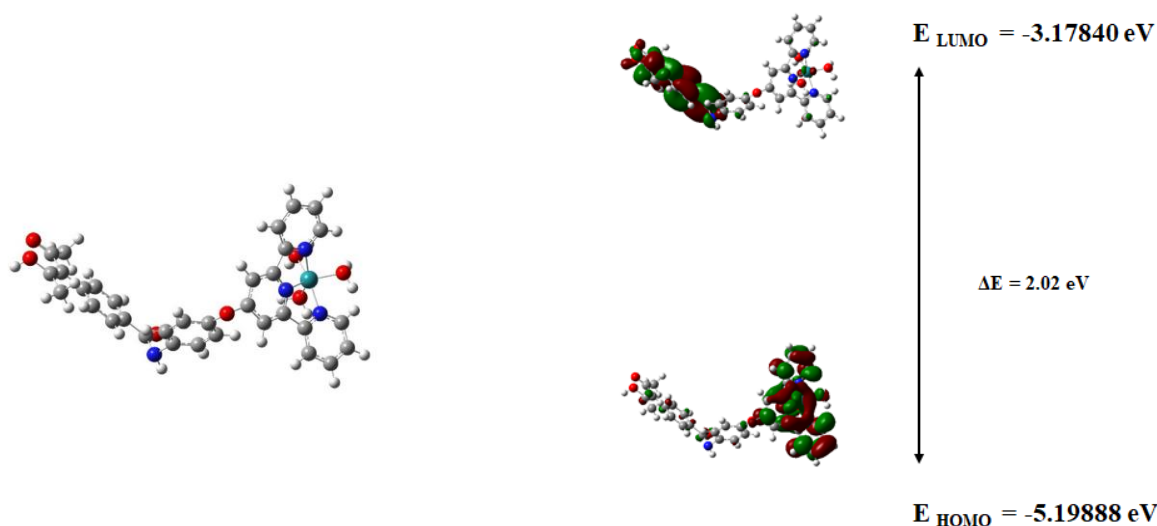


Figure 4. The theoretical optimized geometry of Ru complex

Figure 5. The molecular orbital surfaces for the HOMO and LUMO of Ru complex

The Ru(II) complex (compound **5**) was anchored to nanocrystalline TiO₂ film and the fabricated cell exhibits a short circuit density (J_{sc}) of 12.84 and an open circuit potential (V_{oc}) of 0.69 with efficiency of 4.97% in a DSSC. Table 1 shows the parameters of DSSC made with this Ru complex as a sensitizer. Also the current-voltage characteristic of Ru complex in DSSC was shown in Figure 6.

Table 1. The operation parameters of DSSCs made with new Ru complex as a sensitizer

J_{sc} (mA/cm ²)	V_{oc}	η (%)	FF
12.84	0.69	4.97	0.562

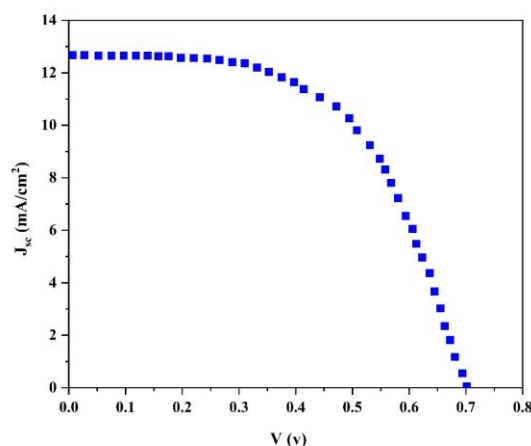


Figure 6. Photocurrent density–voltage (I–V) characteristic curves of the DSSC with this new Ru complex as a sensitizer

The efficiency of this DSSC using this new Ru complex as a sensitizer was compared to some of those reported in the literature using ruthenium complexes as a dye. Also, we were checked the efficiency of N719 dye at the same condition. As can be seen in Table 2 our prepared dye is the most efficient among them.

Table 2. Comparison of the efficiency of different DSSCs using Ru complexes as a dye

Row	Dye (complex)	η %	FF	Ref.
1	polyRu(tpy) ₂ (BF ₄) ₂	0.07	0.29	27
2	[Ru(cptpy)(8-quinolinolate)(NCS)]	0.2	0.64	28
3	[Ru(TAPNB) ₂ (NCS) ₂]	0.25	0.49	27
4	[Ru(quo)(dcbpy) ₂]Cl	1.00	0.66	27
5	[Ru(Me ₂ quo)(dcbpy) ₂]Cl	1.00	0.70	29
6	[Ru(dcbpy) ₂ (L)]PF ₆ L= 9-butyl-3-(thiazol-2-yl)-9H-carbazole	1.02	0.69	30
7	[Ru(dcbpy) ₂ (L)]PF ₆ L=N-phenyl-N-(4-(thiazol-2-yl)phenyl)-benzenamine	1.06	0.66	30
8	[Ru(dcbpy) ₂ (L)]PF ₆ L=N-(4-(benzo[d]thiazol-2-yl)phenyl)-N-phenylbenzenamine	1.40	0.69	30
9	<i>Bis</i> (4'-carboxy-2,2':6',2''-terpyridine)ruthenium(II)	1.56	0.49	31

	<i>bis</i> (hexafluorophosphate)			
10	{(Et) ₃ NH}[Ru(2,2':6',2''-terpyridine-4'-carboxylic acid)(NCS) ₃]	2.48	0.65	32
11	(<i>E</i>)-2-Cyano-3-(5-(7-(4-(diphenylamino)-phenyl)-[1,2,5]thiadiazol[3,4- <i>c</i>]pyridin-4-yl)-thiophen-2-yl)acrylic acid	2.63	0.64	33
12	[Ru(dcbpy) ₂ (L)]PF ₆ L=3-(benzo[<i>d</i>]thiazol-2-yl)-9-butyl-9 <i>H</i> -carbazole	2.98	0.72	30
13	[Ru(4,4',4''-tri- <i>tert</i> -butyl-2,2':6',2-terpyridine)(4,7-diphenyl-1,10-phenanthroline disulfonic acid disodium salt)(thiocyanate)]	3.41	0.57	34
14	(<i>E</i>)-3-(5-(7-(4-(<i>Bis</i> (9,9-dimethyl-9 <i>H</i> -fluoren-2-yl)amino)phenyl)-[1,2,5]thiadiazolo[3,4- <i>c</i>]pyridin-4-yl)thiophen-2-yl)-2-cyanoacrylic acid	3.58	0.69	33
15	Ru(mttpy) ₂ (PF ₆) ₂	3.61	0.57	27
16	Complex 5	4.97	0.562	Present work
17	N719 dye	4.8	0.55	Present work

In summary, a new Ru (II) complex with 4'-functionalized 2,2':6',2''-terpyridine ligand was synthesized by a multistep procedure for dye-sensitized solar cell application. The 4'-functionalized 2,2':6',2''-terpyridine ruthenium complex anchored to the TiO₂ surface acts as a photosensitizer in a nano crystalline dye-sensitized solar cell. Furthermore, the photoelectron chemical properties of complex were investigated. The solar-to-electric conversion efficiency of 4.97% is achieved with this ruthenium dye under the standard AM 1.5 conditions.

EXPERIMENTAL

Materials and methods

All solvents were dried by standard methods and distilled prior to use. Commercially available reagents were used without further purification. All reagents for the chemical synthesis were purchased from Aldrich or Merck chemical companies. ¹H and ¹³C NMR spectra were recorded in CDCl₃ by a Bruker-Avance 400 NMR Spectrometer. UV-Vis spectra were obtained by a JASCO V-670 UV-Vis Spectrophotometer (190–2700 nm). FT-IR spectra were obtained by a JASCO, FT/IR-6300 instrument (400–4000 cm⁻¹). The Gaussian 16 software was used to do all of calculations (geometrical optimization

and electronic transitions). The GaussView6.1 software was used to assign the computed optimized structure and finding the HOMO and LUMO energies.

Synthesis of 4'-(4-aminophenyl)-2,2':6',2''-terpyridine (2)

In a round-bottom flask, 4-aminophenol (103 mg, 0.943 mmol) was added to a suspension of powdered KOH (224 mg, 3.99 mmol) in DMSO (30 mL) at 55 °C and stirred for 30 min. Then, 4'-chloro-2,2':6',2''-terpyridine (**1**, 505 mg, 1.89 mmol) was added to the reaction mixture and stirred at 55 °C for 12 h. At the end of the reaction, the reaction mixture was cooled to room temperature and poured into deionized water (300 mL). The aqueous phase was removed after centrifuging the reaction mixture, and the product was washed with deionized water and dried *in vacuo*. The crude product was dissolved in EtOAc and the insoluble by-product was filtered off. Recrystallization from EtOAc yielded the colorless crystals of compound **2** (Scheme 1). The sample was characterized by FT-IR and ¹H NMR spectroscopy. Compound **2** (Scheme 1) was characterized by FT-IR (Figure S 10) and NMR (Figure S 1, S 2, S 3 and S 4) methods. The amine group appears in the region of 3249 and 3450 cm⁻¹. The C-O band appears in the region 1243 cm⁻¹. The C=C band appears in 1504 cm⁻¹. The C=N band appears in 1585 cm⁻¹.

¹H NMR (CDCl₃, 400 MHz): δ (ppm) = 4.02 (s, 2H, H^{N-H}), 6.60 (d, *J* = 6.2 Hz, 2H, H^{A2}), 6.76 (d, *J* = 2.2 Hz, 2H, H^{A3}), 7.28 (dd, *J* = 4.8, 7.2 Hz, 2H, H^{T5}), 7.78 (dd, *J* = 3.6, 8.8 Hz, 2H, H^{T4}), 8.40 (s, 2H, H^{T3}), 8.51 (d, *J* = 7.4 Hz, 2H, H^{T3}), 8.61 (d, *J* = 4.7 Hz, 2H, H^{T6}).

¹³C NMR (CDCl₃, 100 MHz): 165.8 (C_{T4'}), 155.6 (C_{T2'}), 154.4 (C_{T2}), 149.5 (C_{T6}), 145.0 (C_{A1}), 144.2 (C_{A4}), 137.4 (C_{T4}), 124.3 (C_{T3}), 122.1 (C_{A2}), 121.6 (C_{T5}), 116.8 (C_{A3}), 107.9 (C_{T3'}).

Synthesis of 3-[4-benzoic acid]pentane-2,4-dione (3)

For the synthesis of this compound (compound **3**), we used a reported synthetic method with a little change.^{2,25} First, 2,4-pentanedione (4.5 mmol) was added to a flask containing 4-iodobenzoic acid (1.5 mmol), CuI (0.15 mmol), K₂CO₃ (7.5 mmol) and *L*-proline (0.3 mmol). Then 15 mL of DMSO solvent was added to this mixture and the reaction mixture was heated at 90 °C for one day under nitrogen gas. The solution was allowed to cool and 1 M HCl was added to cooled solution and extracted with EtOAc solvent. Finally, the organic layer was dried with Na₂SO₄. After evaporation of solvent with rotary, the sample was dried under vacuum overnight. The oil product was purified with silica column using hexane/EtOAc (1:1) as eluent (Scheme 2).

Compound **3** (Scheme 2) was characterized by FT-IR (Figure S 11) and NMR (Figure S 5 and S 6) methods. The FT-IR spectrum of compound **3** (Figure S 11) showed an intense absorption band at 1686 cm⁻¹ due to the presence of C=O functional group, while the band observed at 1606 cm⁻¹ corresponds to C=C bond. The stretching vibration of carboxylic acid O-H and the other OH groups appear as a very broadband in the region 2800–3400 cm⁻¹, centered at about 3000 cm⁻¹. The absorption bands at 2999 cm⁻¹ and 3070 cm⁻¹ is assigned to the C-H bonds. These observations proved the structure of compound **3**.

^1H NMR (CDCl_3 , 400 MHz) (100% enol form) δ (ppm) = 16.74 (s, 1H, OH), 8.15 (d, $^3J_{\text{H-H}} = 8$ Hz, 2H, CH_{Ar}), 7.33 (d, $^3J_{\text{H-H}} = 8$ Hz, 2H, CH_{Ar}), 1.91 (s, 6H, CH_3).

^{13}C NMR (CDCl_3 , 100 MHz): 190.7 (C-OH), 171.1 (COOH), 142.8 (C_{Ar}), 131.4 (CH_{Ar}), 130.7 (CH_{Ar}), 128.6 (C_{Ar}), 114.5 (C_{Enol}), 24.2 (CH_3).

Synthesis of *N*-(4-(2,6-di(pyridine-2-yl)pyridine-4-yloxy)phenyl)-4-((*Z*)-2-hydroxy-4-oxopent-2-en-3-yl)benzamide (4)

First, 5 mL of CH_2Cl_2 was added to the three-neck flask containing compound **3** (0.255 mmol). Then, thionyl chloride (0.38 mmol) was added dropwise to the reaction solution under stirring and the reaction mixture was heated to reflux for 4 h. After cooling the solution and evaporation of solvent, dry CH_2Cl_2 (5 mL) and *N,N'*-diisopropylethylamine (0.31 mmol) were added respectively. The reaction mixture was stirred at room temperature for 15 min. Compound **2** (0.255 mmol) was dissolved in dry $\text{CH}_2\text{Cl}_2/\text{EtOAc}$ (2:1), (3 mL) and this solution was added to reaction solution. The orange solution was heated for one more day. The solution was allowed to cool and the water was added to cooled solution and extracted with EtOAc. The organic layer was washed with saturated aqueous NaHCO_3 solution and was dried with Na_2SO_4 . After evaporation of solvent, the oily product was purified with silica column with $\text{MeOH}/\text{CH}_2\text{Cl}_2$ (1:100) as eluent and final with MeOH/EtOAc (1:100) for further elution for removing an orange band containing compound **4** (Figure 3). The ligand was characterized by FT-IR, ^1H NMR and ESI-MS techniques.

The structure of compound **4** (Scheme 3) was confirmed by ESI-MS, NMR (Figure S 7, S8 and S9), and FT-IR (Figure S 12). ESI-MS: *m/z* ($\text{C}_{33}\text{H}_{26}\text{N}_4\text{O}_4$), Found: 542.6, Calculated: 542.6. In the FT-IR spectrum of compound **4** (Figure S 12), the C=O stretching band of the amide group and C=O carbonyl group appeared at 1730 cm^{-1} . The band at $3300\text{--}3429\text{ cm}^{-1}$ was assigned to NH of amide group, and the hydroxyl group stretching band. The absorption band at 2854 cm^{-1} and 2925 cm^{-1} was due to the C-H bonds.

^1H NMR ($\text{DMSO-}d_6$, 400 MHz): δ (ppm) = 1.92 (s, 3H, CH_3'), 1.99 (s, 3H, CH_3), 6.68 (d, $J = 8.8$ Hz, 2H, $\text{H}^{\text{A}2}$), 6.90 (d, $J = 1.2$, 2H, $\text{H}^{\text{L}2}$), 6.91 (d, $J = 8.8$ Hz, 2H, $\text{H}^{\text{A}3}$), 7.48 (dd, $J = 5.2, 6.1$ Hz, 2H, $\text{H}^{\text{T}5}$), 7.70 (d, $J = 1.6$ Hz, 2H, $\text{H}^{\text{L}1}$), 7.71 (s, 1H, $\text{H}^{\text{N-H}}$), 7.88 (s, 2H, $\text{H}^{\text{T}3}$), 7.99 (dd, $J = 1.6, 7.6$ Hz, 2H, $\text{H}^{\text{T}4}$), 8.59 (d, $J = 8$ Hz, 2H, $\text{H}^{\text{T}3}$), 8.71 (d, $J = 4.8$ Hz, 2H, $\text{H}^{\text{T}6}$), 13.78 (s, 1H, H^{OH}).

^{13}C NMR (CDCl_3 , 100 MHz): 191.8 ($\text{C}_{\text{M}2}$), 172.4 ($\text{C}_{\text{M}4}$), 165.9 ($\text{C}_{\text{T}4'}$), 164.7 (C_{amide}), 155.3 ($\text{C}_{\text{T}2'}$), 154.6 ($\text{C}_{\text{T}2}$), 150.4 ($\text{C}_{\text{A}1}$), 149.4 ($\text{C}_{\text{T}6}$), 137.5 ($\text{C}_{\text{T}4}$), 136.1 ($\text{C}_{\text{L}3}$), 133.3 ($\text{C}_{\text{L}6}$), 131.9 ($\text{C}_{\text{A}4}$), 127.3 ($\text{C}_{\text{L}1}$), 126.9 ($\text{C}_{\text{L}2}$), 124.2 ($\text{C}_{\text{T}3}$), 123.9 ($\text{C}_{\text{A}3}$), 121.8 ($\text{C}_{\text{A}2}$), 121.3 ($\text{C}_{\text{T}5}$), 108.9 ($\text{C}_{\text{M}3}$), 107.7 ($\text{C}_{\text{T}3'}$), 26.8 ($\text{C}_{\text{M}1}$), 17.2 ($\text{C}_{\text{M}5}$).

Synthesis of ruthenium(II) complex (5)

The Ru complex was prepared in a microwave oven. A suspension of the compound **4** (1 mmol) and

$\text{RuCl}_3 \cdot 3\text{H}_2\text{O}$ (1 mmol) in ethylene glycol (5 mL) was heated in a microwave oven at 600 W for 15 min. Then the red solution was poured into water (40 mL), $[\text{NH}_4][\text{PF}_6]$ (5 g) was added, the desired complex was filtered over Celite, washed with water and Et_2O successively and dried. The complex was then dissolved in MeCN and solvent was removed. Upon recrystallization by diffusion of Et_2O into the MeCN solution, compound **5** was obtained (Figures **1a** and **1b**). The complex was characterized by UV-vis, ESI-MS and CHN analysis techniques. ESI-MS: m/z , ($\text{RuC}_{33}\text{H}_{32}\text{N}_4\text{O}_7$), Found: 697.7923, Calculated: 697.6934. CHN analysis of compound obtained: Anal. Calcd For $\text{RuC}_{33}\text{H}_{32}\text{N}_4\text{O}_7$: C, 56.80; H, 4.63; N, 8.03. Found: C, 56.83; H, 4.61; N, 8.05 %.

This complex was used as a photosensitizer for manufacturing of dye-sensitized solar cells, and finally, the current-voltage curve and also efficiency of these cells were measured.

TiO₂ thin film preparation

TiO₂ paste (average particle size about 13 nm) was purchased from Solaronix Company. TiO₂ thin film was prepared by the doctor blade procedure. We used Scotch tape and a glass rod to spread a drop of viscous TiO₂ suspension onto a microscope glass slip to obtain a mesoporous film of uniform thickness. After tape removal and air drying for approximately 1 h at room temperature, it was sintered for 30 min at 450 °C to form a transparent TiO₂ thin film (The thickness of TiO₂ thin film was 2 μm and the area of the TiO₂ thin film is 0.25 cm²). By soaking the still hot (80 °C) film in the synthesized Ru complex (0.5 mM in MeCN solvent), dye sensitization of the TiO₂ film was carried out and incubated for around 48 h at room temperature. The film was rinsed with EtOH several times after the sensitization process to wash off the unattached dye, covered with EtOH and another slip of microscope glass, and eventually sealed. Dye-sensitized films were prepared and kept in the dark before measurement (Figure 2).

Cell assemble

A sandwich cell was prepared using the dye anchored TiO₂ film as a working electrode and a second conducting glass coated with chemically deposited platinum from 0.05 M hexachloroplatinic acid as a counter electrode. The transparent film of the Surlyn polymer was superimposed on the two electrodes. The superimposed electrodes were tightly held and applied heat (120 °C) around the Surlyn to seal the two electrodes. The electrolyte consists of 0.6 M 1,2-dimethyl-3-propylimidazolium iodide, 0.05 M I₂, 0.1 M lithium iodide, and 0.5 M 4-*tert*-butylpyridine was prepared in acetonitrile solvent and used simultaneously. A drop of electrolyte solution was introduced into the electrode space from the counter electrode side through a pre-drilled hole. Then, the drilled hole was sealed with microscope cover slide and Surlyn to prevent leakage of the electrolyte solution. The current-voltage (I-V) curves of the dye-sensitized solar cells were measured with μ-Autolab type III (Ecovchemie, Utrecht, the Netherlands) controlled by a microcomputer with Nova 1.7 software, under illumination of 100 mWcm⁻² using the solar simulator (Luzchem, V 1.2) equipped with a water-based IR filter.

SUPPLEMENTARY INFORMATION (SI)

The NMR data for all of compound and also FT-IR of them are available in supplementary section.

ACKNOWLEDGEMENTS

The support of this work by the University of Isfahan is acknowledged.

REFERENCES

1. S. G. Abuabara, C. W. Cady, J. B. Baxter, C. A. Schmuttenmaer, R. H. Crabtree, G. W. Brudvig, and V. S. Batista, *J. Phys. Chem. C*, 2007, **111**, 11982.
2. W. R. McNamara, R. C. Snoeberger III, G. Li, J. M. Schleicher, C. W. Cady, M. Poyatos, C. A. Schmuttenmaer, R. H. Crabtree, G. W. Brudvig, and V. S. Batista, *J. Am. Chem. Soc.*, 2008, **130**, 14329.
3. B. O'Regan and M. Grätzel, *Nature*, 1991, **353**, 737.
4. A. Nasirian, V. Mirkhani, M. Moghadam, S. Tangestaninejad, and I. Mohammadpour-Baltork, *J. Chem. Sci.*, 2020, **132**:75, 1.
5. P. R. Andres, R. Lunkwitz, G. R. Pabst, K. Böhn, D. Wouters, S. Schmatloch, and U. S. Schubert, *Eur. J. Org. Chem.*, 2003, 3769.
6. G. R. Newkome, E. He, and L. A. Godínez, *Macromolecules*, 1998, **31**, 4382.
7. G. R. Newkome, K. S. Yoo, and C. N. Moorefield, *Chem. Commun.*, 2002, **18**, 2164.
8. H. Jiang, S. J. Lee, and W. Lin, *Org. Lett.*, 2002, **4**, 2149.
9. U. S. Schubert and C. Eschbaumer, *Angew. Chem. Int. Ed.*, 2002, **41**, 2892.
10. B. G. G. Lohmeijer and U. S. Schubert, *Angew. Chem. Int. Ed.*, 2002, **41**, 3825.
11. S. Kelch and M. Rehahn, *Macromolecules*, 1999, **32**, 5818.
12. A. Khatyr and R. Ziessel, *J. Org. Chem.*, 2000, **65**, 3126.
13. J. F. Gohy, B. G. G. Lohmeijer, S. K. Varshney, and U. S. Schubert, *Macromolecules*, 2002, **35**, 7427.
14. M. K. Nazeeruddin, P. Péchy, T. Renouard, S. M. Zakeeruddin, R. Humphry-Baker, P. Comte, P. Liska, L. Cevey, E. Costa, V. Shklover, L. Spiccia, G. B. Deacon, C. A. Bignozzi, and M. Grätzel, *J. Am. Chem. Soc.*, 2001, **123**, 1613.
15. M. K. Nazeeruddin S. M. Zakeeruddin, R. Humphry-Baker, T. A. Kaden, and M. Grätzel, *Inorg. Chem.*, 2000, **39**, 4542.
16. T. Fukuo, H. Monjushiro, H.-G. Hong, M.-A. Haga, and R. Arakawa, *Rapid Commun. Mass Spectrom.*, 2000, **14**, 1301.
17. A. H. L. Goff, S. Joiret, and P. Falaras, *J. Phys. Chem. B*, 1999, **103**, 9569.

18. S. M. Zakeeruddin, M. K. Nazeeruddin, P. Pechy, F. P. Rotzinger, R. Humphry–Baker, K. Kalynasundaram, M. Grätzel, V. Shklover, and T. Haibach, *Inorg. Chem.*, 1997, **36**, 5937.
19. M. Grätzel, O. Kohle, M. K. Nazeeruddin, P. Pechy, F. P. Rotzinger, S. Ruile, and S. M. Zakeeruddin, 1995, *WO 9529924*.
20. P. Péchy, F. P. Rotzinger, M. K. Nazeeruddin, O. Kohle, S. M. Zakeeruddin, R. Humphry–Baker, and M. Grätzel, *J. Chem. Soc., Chem. Commun.*, 1995, 65.
21. M. C. DeRosa, F. Al–Mutlaq, and R. J. Crutchley, *Inorg. Chem.*, 2001, **40**, 1406.
22. E. C. Constable, P. Harverson, and J. J. Ramsden, *J. Chem. Soc., Chem. Commun.*, 1997, 1683.
23. K. W. Cheng, C. S. C. Mak, W. K. Chan, A. M. Ching Ng, and A. B. Djurišić, *J. Polym. Sci. A: Polym. Chem.*, 2008, **46**, 1305.
24. P. A. Anderson, G. F. Strouse, J. A. Treadway, F. R. Keene, and T. J. Meyer, *Inorg. Chem.*, 1994, **33**, 3863.
25. Y. W. Jiang, N. Wu, H. H. Wu, and M. Y. He, *Synlett*, 2005, 2731.
26. A. Nasirian, V. Mirkhani, M. Moghadam, S. Tangestaninejad, and I. Mohammadpour–Baltork, *J. Iran. Chem. Soc.*, 2015, **12**, 529.
27. A. Anthonysamy, S. Balasubramanian, B. Muthuraaman, and P. Maruthamuthu, *Nanotechnology*, 2007, **18**, 095701.
28. J. A. Bonacin, S. H. Toma, J. N. Freitas, A. F. Nogueira, and H. E. Toma, *Inorg. Chem. Commun.*, 2013, **36**, 35.
29. C. Dragonetti, A. Valore, A. Colombo, M. Magni, P. Mussini, D. Roberto, R. Ugo, A. Valsecchi, V. Trifiletti, N. Manfredi, and A. Abbotto, *Inorg. Chim. Acta*, 2013, **405**, 98.
30. C. H. Siu, C. L. Ho, J. He, T. Chen, X. Cui, J. Zhao, and W. Y. Wong, *J. Organomet. Chem.*, 2013, **748**, 75.
31. A. Sepehrifard, S. Chen, A. Stublla, P. G. Potvin, and S. Morin, *Electrochim. Acta*, 2013, **87**, 236.
32. G. C. Vougioukalakis, T. Stergiopoulos, G. Kantonis, A. G. Kontos, K. Papadopoulos, A. Stublla, P. G. Potvin, and P. Falaras, *J. Photochem. Photobiol. A: Chem.*, 2010, **214**, 22.
33. Y. Hua, H. Wang, X. Zhu, A. Islam, L. Han, C. Qin, W. Y. Wong, and W. K. Wong, *Dyes Pigm.*, 2014, **102**, 196.
34. S. Erten–Ela, S. Sogut, and K. Ocakoglu, *Mater. Sci. Semicond. Process.*, 2014, **23**, 159.